Available online at www.sciencedirect.com
SCIENCE DIRECT®

Journal of the European Ceramic Society 24 (2004) 2989–2994

www.elsevier.com/locate/jeurceramsoc

Internal friction in hard and soft PZT-based ceramics

H. Frayssignes[a,*], M. Gabbay[a], G. Fantozzi[a], N.J. Porch[b], B.L. Cheng[c], T.W. Button[b]

[a]*GEMPPM UMR CNRS 5510, INSA de Lyon, 69621 Villeurbanne Cedex, France*
[b]*IRC in Materials Processing, University of Birmingham, Edgbaston B15 2TT, UK*
[c]*Institute of Physics, Chinese Academy of Sciences, Beijing 100080, China*

Received 16 March 2003; received in revised form 17 October 2003; accepted 25 October 2003

Abstract

This study concerns the two following commercial ceramics: PZT TRS100 (US Navy I standard: hard material) and PZT TRS600 (US Navy VI standard: soft material). These materials are PZT ceramics with various dopants. Internal friction and elastic modulus measurements have been performed versus temperature at different frequencies. Considering the hard ceramic, two relaxation peaks (R_1, R_2) related to oxygen vacancies–domain walls interaction were observed similarly to undoped PZT ceramics. In addition, a phase transition peak (P_1) occurs at the Curie temperature. Considering the soft ceramic, only two phase transition peaks were observed. The increase of modulus associated with the phase transition internal friction peak occurs at the Curie temperature in both samples. The effects of some dopants are investigated. Some of them influence either the concentration of oxygen vacancies or the domains structure.

Keywords: Ferroelectric properties; Internal friction; Mechanical properties; Perovskites; PZT

1. Introduction

Piezoelectric materials are widely used for applications in microelectronics or power transducers. Lead zirconate titanate ceramic (PZT) is the most used because of a formulation close to the morphotropic phase boundary, rhombohedral and tetragonal phases coexist and optimal piezoelectric coefficients[1,2] are reached. Undoped PZT ceramics are seldom used. They are usually substituted in the A-sites or/and in the B-sites of the perovskite structure ABO_3 in order to improve dielectric, piezoelectric and mechanical properties. Considering their properties the classification in two families "hard materials" or "soft materials" is conventionally used.

Since the internal friction is very sensitive to the microstructure of materials, the doping effects can be studied by mechanical spectrometry. Both doping effects[3] and those of the Zr/Ti ratio[4,5] have been reported in recent studies of internal friction for PZT-based ceramics. In the most cases, two relaxation peaks of internal friction located in the ferroelectric phase have been observed and they were noted *R*. They were attributed to the interaction of point defects with domain walls. In addition, it has been observed that each phase transition induces an internal friction peak associated with an anomaly of elastic modulus. The loss peak of the phase transition and the modulus anomaly were noted *P* and *M*, respectively.

The aim of this paper is to investigate and compare the internal friction behaviour of a "hard" ceramic (PZT TRS100) and a "soft" ceramic (PZT TRS600) both manufactured by TRS Ceramics Inc. The peculiarity of this work lies in the comparison of two substituted PZT materials having a Zr/Ti ratio near the morphotropic phase boundary. At room temperature, PZT TRS100 shows lower dielectric (0.5%) and mechanical ($<0.2\%$) losses than PZT TRS600[6] (dielectric and mechanical losses about 2%).

Starting with manufactured powders, the first part describes the different processing stages to obtain the final parallelepiped specimens. Compared with conventional processing, the main change occurs during a special mixing with a polymer binder.

* Corresponding author. Tel.: +33-47243-8498; fax: +33-47243-8528.
E-mail address: frayssignes@yahoo.fr (H. Frayssignes).

0955-2219/$ - see front matter © 2003 Elsevier Ltd. All rights reserved.
doi:10.1016/j.jeurceramsoc.2003.10.048

The elastic modulus and internal friction measurements are reported in the second part. The internal friction dependence with the temperature underlines the occurrence of phase transitions and/or relaxation processes due to the motions of domain walls. The comparison of hard and soft materials helps to understand the doping effects in PZT ceramics.

1.1. Processing

According to TRS Ceramics Inc.'s information, the chemical formulation for PZT TRS100 material can be represented as $Pb_{96.2}Sr_{3.8}$ $(Zr_{51.8}, Ni_{0.8},Fe_{0.8},Ti_{46.6})O_3$ since Fe^{3+} and Ni^{2+} ions reach the B-sites and Sr^{2+} ions occupy the A-sites of the perovskite structure. The PZT TRS600 with chemical formulation $Pb_{90.6}La_{9.4}$ $(Zr_{49.7},Ti_{44.7},Sn_{5.6})O_3$ is commonly called PLZT. Commercial PZT TRS600 and PZT TRS100 powders have respectively, an average grain size of 1.8 and 3.5 μm. The samples were prepared according to the viscous polymer processing (VPP) route. Powders were firstly blended with a polymer binder in order to obtain a paste, which was secondly mixed in a twin roll mill (Interdisciplinary Research Centre, University of Birmingham, United Kingdom); a final lamination makes it possible to obtain sheets of 1.3–1.4 mm in thickness. Samples with dimensions 55×5×1.3 mm were sliced up from the dried paste. To remove additive polymer, samples were initially fired up to 500 °C at a heating rate of 30 °C/h before sintering (in a lead zirconate atmosphere) at 1200 °C during 30 min with a heating rate of 10 °C/min.

The absolute densities for PZT TRS600 and PZT TRS100 were about 7.31 and 7.41 g/cm^3, respectively. The microstructures of the two PZT are shown in Figs. 1 and 2 for the PZT TRS 100 and TRS 600, respectively. The grain size is homogenous in PZT TRS 600, but it is not the case for the PZT TRS 100.

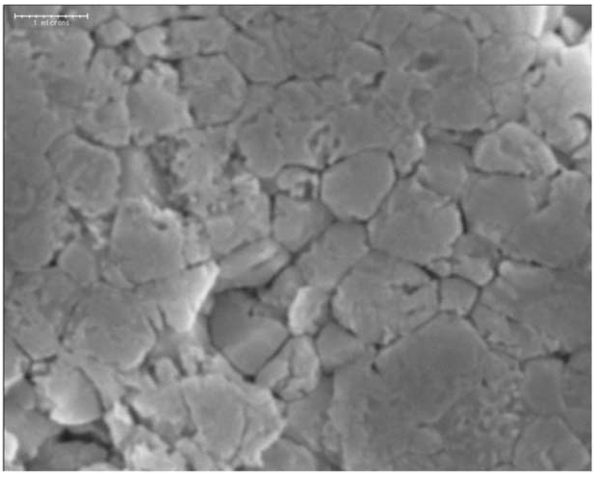

Fig. 1. Scanning electron micrograph of PZT TRS100.

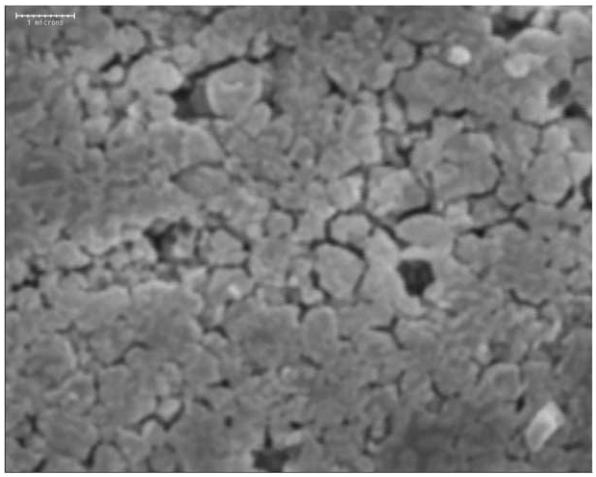

Fig. 2. Scanning electron micrograph of PZT TRS600.

Silver electrodes were deposited on some samples and fired at 600 °C during 1 h in order to measure the damping in the kilohertz frequency range.

2. Internal friction of PZT ceramics

In the low frequency range (<1 Hz), internal friction (Q^{-1}) and shear modulus (G) were simultaneously measured versus temperature with a forced pendulum.[7] Internal friction is deduced from the loss angle between applied stress and resulting strain. Shear modulus corresponds to the stress/strain ratio. The strain amplitude was about 10^{-6}.

At a medium frequency (2–3 kHz), internal friction (Q^{-1}) and Young's modulus (E) were simultaneously recorded versus temperature with another device,[7] which makes it possible to drive (electrostatically) the specimen in flexural vibration at its resonance frequency.[8] Young's modulus and internal friction are determined from the resonance curve (amplitude response versus frequency) at a given temperature.

All measurements were performed at a heating rate of 1 °C/min in vacuum.

2.1. PZT TRS100 ceramic

Fig. 3 shows the variation of $Q^{-1}(T)$ in the low-frequency range. Three peaks R_1, R_2 and P_1 appear. Those peaks cannot be accurately determined because of their overlapping. With increasing frequency, the temperatures of the R_1 and R_2 peaks increase whereas the P_1 peak temperature (304 °C) is not frequency dependent. Fig. 4 shows the variation of $G(T)$ in the low-frequency range. Three modulus anomalies M_1, A_1 and A_2 appear corresponding to the P_1, R_1 and R_2 peaks, respectively. With increasing temperature, the shear modulus increases from the M_1 temperature. The phase reaches

gradually the cubic phase so the anomaly M_1 appears close to the Curie temperature. The P_1 peak is therefore associated with the phase transformation from tetragonal (ferroelectric) to cubic (paraelectric) at the Curie temperature (T_C).[4]

Fig. 5 shows $E(T)$ and $Q^{-1}(T)$ curves in the kilohertz frequency range. A modulus anomaly M_1 appears close to the Curie temperature (T_C). Above T_C, the modulus increases progressively showing a smooth phase transition. A broad R' peak (about 290 °C) is obtained close to the temperature of the anomaly M_1.

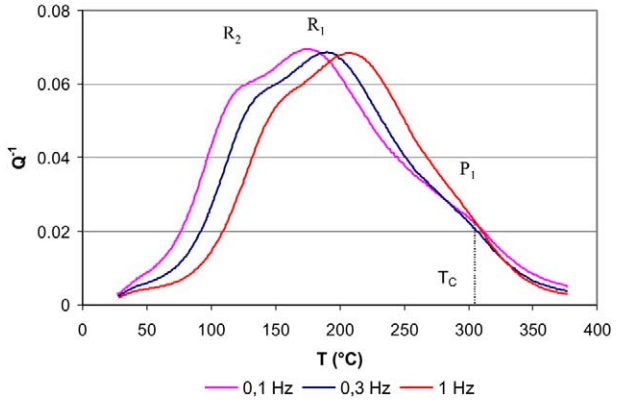

Fig. 3. Variation of internal friction Q^{-1} with temperature for different frequencies (PZT TRS100).

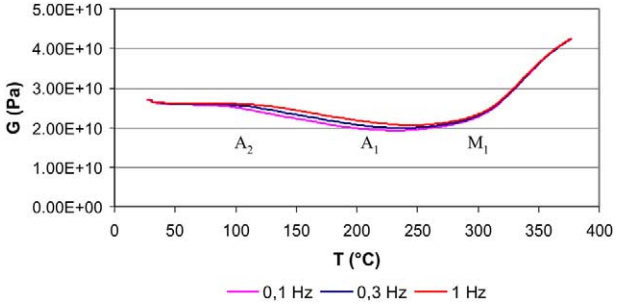

Fig. 4. Variation of shear modulus G with temperature for different frequencies (PZT TRS100).

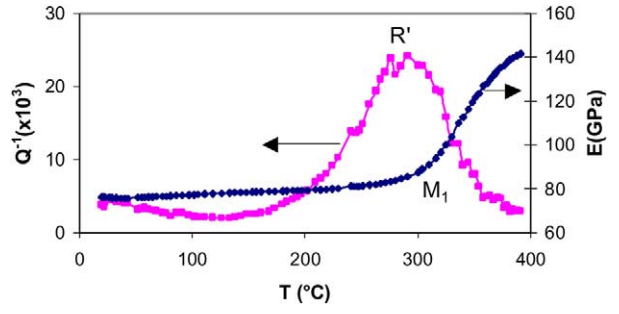

Fig. 5. Variation of internal friction Q^{-1} and Young's modulus E with temperature in the kHz frequency range (PZT TRS100).

2.2. PZT TRS600 ceramic

Fig. 6 shows the variation of $Q^{-1}(T)$ in the low-frequency range. A broad P_1 peak appears at 188 °C and another small one called P_2 appears near 70 °C. The P_1 and P_2 peak temperatures are not frequency dependent so they correspond to different phase transitions. Fig. 7 shows the variation of $G(T)$ in the low-frequency range. Two modulus anomalies called M_1 and M_2 correspond to the P_1 and P_2 peaks, respectively. From the M_1 modulus anomaly, the shear modulus increases with increasing temperature. The ferro–paraelectric (cubic) phase transition occurs at the M_1 temperature, which is close to the Curie temperature (T_C).

Fig. 8 shows $E(T)$ and $Q^{-1}(T)$ curves in the kilohertz frequency range. Despite an important background loss (dashed line), two peaks P_2 (about 80 °C) and P_1 (about 166 °C) appear and they correspond to the different phase transitions as it can be seen in the low-frequency case. Previous works[9] have shown that the magnitudes of those phase transition peaks were proportional to the reciprocal frequency. That might explain the weak magnitudes of peaks and the important background loss in the kilohertz frequency range. The Young's modulus

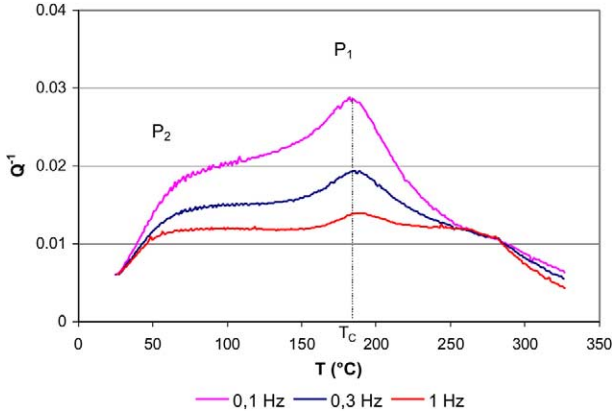

Fig. 6. Variation of internal friction Q^{-1} with temperature for different frequencies (PZT TRS600).

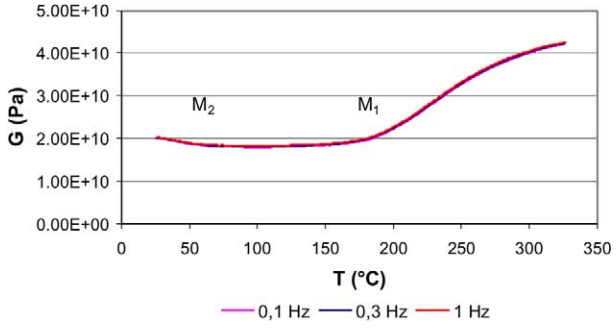

Fig. 7. Variation of shear modulus G with temperature for different frequencies (PZT TRS600).

anomaly called M_1 is identified near the P_1 peak temperature so near the Curie temperature (T_C). Above T_C, the modulus increases progressively showing a smooth phase transition towards cubic phase (paraelectric).

3. Discussion

The modulus and internal friction measurements applied on doped[3,5,9,10] and undoped[4] PZT piezoelectric ceramics have shown modulus anomalies, relaxation and phase transition peaks. In addition to the P_1 peak related to the ferro–paraelectric phase transition, a P_2 peak related to the rhombohedral–tetragonal phase transition has been observed in some PZT based ceramics.[7] In the following section, bibliographic results help to investigate the different causes of mechanical loss generation, and the doping effects are discussed.

3.1. PZT TRS100 ceramic

The R_2 and R_1 peaks are frequency dependent (Fig. 3) so they are controlled by relaxation processes. The calculation of their activation parameters with the Arrhenius plots (Fig. 9) help to determine the nature of

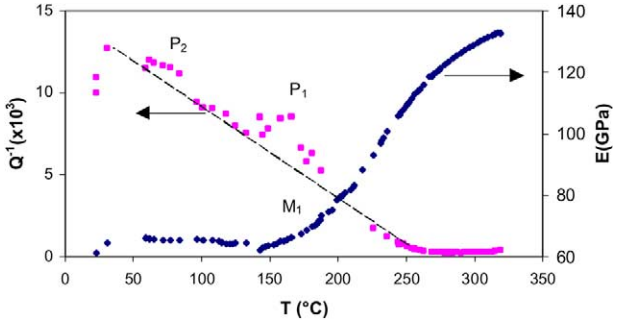

Fig. 8. Variation of internal friction Q^{-1} and Young's modulus E with temperature in the kHz frequency range (PZT TRS600).

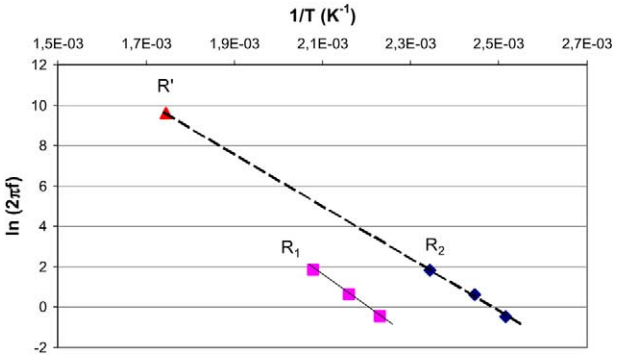

Fig. 9. Arrhenius plot (PZT TRS100).

relaxation processes. Activation energy (H) and relaxation limit time (τ_o) are linked as:[11]

$$\tau = \tau_o \exp(H/kT)$$

where T is the absolute temperature and k the Boltzmann constant.

R_2 and R_1 peaks are considered as two Debye peaks so $\omega\tau = 1$ ($\omega = 2\pi f$). This gives:

$$\ln(2\pi f) = -\ln(\tau_o) - H/kT_p$$

T_p corresponds to the temperature of peak maximum.

The results reported in Table 1 are close to ones obtained with undoped[4] and doped lead zirconate titanate.[3,5,10]

At the kilohertz frequency range, the R_1 and R_2 peaks are not observed since only a broad R' peak is obtained (Fig. 5). It might be associated either with the ferroelectric–paraelectric phase transition or with the shift of R_1 and R_2 peaks towards higher temperatures. From the Arrhenius plot, it can be deduced that the R_1 and R_2 peaks should be shifted above the Curie temperature and near 295 °C, respectively. Fig. 9 shows clearly the R_2 peak is connected to the R' peak. The broad R' peak could be also ascribed to the existence of a ferroelectric–paraelectric phase transition peak. Since the magnitude of a phase transition peak is proportional to the reciprocal frequency, the broad R' peak could be only generated by the mechanism of the R_2 peak.

The relaxation R_2 peak has been already observed with undoped[4] and doped lead zirconate titanate with cobalt[5] doping in the B-sites. The activation energy of R_2 peak is close to the one for oxygen vacancies diffusion (0.9 eV). It is concluded that this peak is a pure relaxation mechanism controlled by the interaction between domain walls and oxygen vacancies. In PZT TRS100, Fe^{3+} and Ni^{2+} ions have a lower valence compared with the host ion (B-sites) so they have an acceptor character. To maintain charge neutrality, oxygen vacancies are created in the lattice.

The R_1 peak is more complex to investigate since Bourim et al.[12] have shown the dependence of its height with stress amplitude and heating rate. It is concluded that it could be due to three mechanisms: relaxation, hysteresis and a last one linked to the ferro–paraelectric phase transition. As the activation energy of the R_1 peak is higher than that for oxygen vacancies diffusion,

Table 1
Activation energy and relaxation limit time from the Arrhenius plot

	H (eV)	τ_o (s)
Peak R_1	1.3	2.6×10^{-15}
Peak R_2	1.1	1.0×10^{-14}

it might be attributed to the interaction of domain walls with cation vacancies[13,14] (Zr, Ti). The R_1 peak magnitude depends on the grain size[5] or ferroelectric domain size since domain size is proportional to the square root of the grain size.[15] In our case, the R_1 peak ought to disappear in view of the small grain size (about 1 μm).

3.2. PZT TRS600 ceramic

In this section, the discussion is focused on the La doping effect. Similarly to our case, $Q^{-1}(T)$ curves on PLZT 6/60/40 show two peaks of phase transitions.[9] Previous results[16] on PLZT x/65/35 (x at.% La) have associated those P_2 and P_1 peaks to the rhombohedral1–rhombohedral2 and rhombohedral2 (ferroelectric)–cubic (paraelectric) phase transitions, respectively. The substitution of lead by lanthanum ions involves a decrease[17] of the Curie temperature in the PZT solid solution. It has been shown that lanthanum content above 8 at.% implies a smooth para–ferroelectric phase transition and the dielectric permittivity as a function of temperature can be described by a quadratic Curie's law.[17] Fig. 10 reports the temperature dependence of internal friction on heating and cooling showing a hysteretic effect. Dielectric constant and dissipation factor measurements versus temperature on PLZT 10/53/47 have led to similar results[18] so the thermal hysteretic effect is associated with the relaxor–ferroelectric transition.

As La^{3+} ions substitute Pb^{2+} ions, they possess a donor effect. Lanthanum substitution leads to a decrease of oxygen vacancies in order to maintain charge neutrality. That can explain the absence of relaxation peaks (as seen in Fig. 6). This conclusion is consistent with previous results[5] showing the decrease of R_2 peak with increasing lanthanum content.

The increase of La content in La-doped PZT[18] reduces the domain size so nanometer-sized domains can be obtained. As grain size and domain size obey roughly a parabolic relation,[15] lanthanum inhibits the grain growth. Having smaller grains, R_1 peak disappears due to the strong pinning effect of grain boundaries on domain walls.[19,20] This shows that the R_1 peak is related to the domain (grain) size.

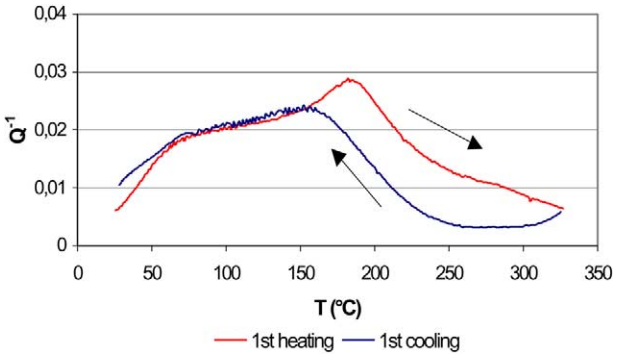

Fig. 10. Internal friction (Q^{-1}) response for PZT TRS600 taken during heating and subsequent cooling at 0.1 Hz.

4. Conclusion

The viscous polymer processing (VPP) route shows possibilities for ceramics processing since the forming stage makes it possible to obtain different complex shapes. This method has been used for obtaining samples in rectangular bars in order to report mechanical spectrometry measurements. The internal friction and elasticity modulus have been investigated on hard and soft PZT-based ceramics.

Internal frictions of PZT TRS100 (hard) versus temperature have shown the R_1 and R_2 relaxation peaks and the P_1 peak. P_1 peak corresponds to a ferroelectric–paraelectric phase transition. R_2 and R_1 peaks are related respectively to the interaction between domain walls–oxygen vacancies and the interaction between domain walls and probably cation vacancies (Zr, Ti).

Internal frictions of PZT TRS600 (soft) versus temperature have shown two peaks called P_2 and P_1. Those peaks can be ascribed to rhombohedral1–rhombohedral2 and rhombohedral2 (ferroelectric)–cubic (paraelectric) phase transitions, respectively. The substitution of lanthanum in the A-sites of the perovskite structure induces the decrease of the Curie temperature (190 °C), oxygen vacancies concentration, domain size and grain size.

Currently, the mechanisms controlling the R_1 peak are not clearly identified. Further investigations on hard materials should be performed for various stress amplitudes, heating rates and chemical formulations to identify clearly the mechanisms responsible of its generation.

Acknowledgements

The samples were prepared at the IRC in Materials Processing (UK) and the internal friction measurements were carried out at the laboratory GEMPPM (France). The authors would like to thank French EGIDE and British Council for the financial support of Alliance Partnership Programme 2002, Project No: 04015YC and PN 02.006.

References

1. Jaffe, B., Cook, W. R. and Jaffe, H., *Piezoelectric Ceramics*. Academic Press, London, 1971.
2. Uchino, K., Ferroelectric ceramics. In *Materials Science and Technology, Vol. 11, Structure and Properties of Ceramics*, ed. M. Swain. VCH, Weinheim, 1994, pp. 635–677.

3. Bouzid, A., Gabbay, M. and Fantozzi, G., Potassium doping effect on the anelastic behaviour of lead zirconate titanate PZT near the morphotropic phase boundary. *Defects and diffusion in ceramics*, 2002, **206**, 147–150.
4. Bourim, E. M., Idrissi, M. H., Cheng, B. L., Gabbay, M. and Fantozzi, G., Elastic modulus and mechanical loss associated with phase transitions and domain walls motions in PZT based ceramics. *J. Phys. IV*, 1996, **6**, C8-633–C8-636.
5. Wang, C., Fang, Q. F. and Zhu, Z. G., Internal friction study of $Pb(Zr,Ti)O_3$ ceramics with various Zr/Ti ratios and dopants. *J. Phys. D: Appl. Phys.*, 2002, **35**, 1545–1549.
6. Gonnard, P., Mise en œuvre et performances des matériaux piézoélectriques. In *Proceedings of the 1er Colloque sur les matériaux électroactifs et leurs applications en génie électrique*, ed. ENSEEIHT. Toulouse, 1998, pp. 15–28.
7. Schaller, R., Fantozzi, G. and Gremaud, G., *Mechanical Spectroscopy Q^{-1} 2001 with Applications to Materials Science*. Trans Tech Publications, Switzerland, 2001.
8. Zener, C., *Elasticité et anélasticité des métaux*. Dunod, Paris, 1955.
9. Cheng, B. L., Gabbay, M., Gimenez, M. and Fantozzi, G., Mechanical loss and elastic modulus associated with phase transitions in PLZT ceramics. *J. Phys. IV*, 1996, **6**, C8-687–C8-690.
10. Postnikov, V. S., Pavlov, V. S., Gridnev, S. A., Turkov, S. K., Darinskii, B. M. and Glosman, I. A., Internal friction in $Pb_{0.96}Sr_{0.05}(Zr_{0.53}Ti_{0.47})O_3 + 3\%PbO$. *Izv. AN SSSR ser. Fizich*, 1967, **31**, 1845–1849.
11. Nowick, A. S. and Berry, B. S., *Anelastic Relaxation in Crystalline Solids*. Academic Press, New York, 1972 (Chapter 3).
12. Bourim, El M., Tanaka, H., Gabbay, M., Fantozzi, G. and Cheng, B. L., Domain wall motion effect on the anelastic behavior in lead zirconate titanate piezoelectric ceramics. *J. Appl. Phys.*, 2002, **91**(10), 6662–6669.
13. Postnikov, V. S., Pavlov, V. S., Gridnev, S. A. and Turkov, S. K., Interaction between 90° domain walls and point defects of the crystal lattice in ferroelectric ceramics. *Sov. Phys.-Solid State*, 1968, **10**(6), 1267–1270.
14. Postnikov, V. S., Pavlov, V. S. and Turkov, S. K., Internal friction in ferroelectrics due to interaction of domain boundaries and point defects. *J. Phys. Chem. Solids*, 1970, **31**, 1785–1791.
15. Cao, W. and Randall, C. A., Grain size and domain size relations in bulk ceramic ferroelectric materials. *J. Phys. Chem. Solids*, 1996, **57**, 1499–1505.
16. Sasaki, Y., Yokosuka, M. and Ochiai, *Japanese J. of Applied Physics*, 1989, **28**(Sup. 28–2), 139–142.
17. Pelaiz Barranco, A., Calderon Pinar, F. and Pérez Martinez, O., Phase transitions in $(Pb,La)Zr_{0.53}Ti_{0.47}O_3$ ferroelectric ceramics. *High Temperatures–High Pressures*, 2000, **32**, 227–232.
18. Gupta, S. M., Li, J. F. and Viehland, D., Coexistence of relaxor and normal ferroelectric phases in morphotropic phase boundary compositions of lanthanum-modified lead zirconate titanate. *J. Am. Ceram. Soc.*, 1998, **81**, 557–621.
19. Arlt, G., Twinning in ferroelectric and ferroelastic ceramics: stress relief. *J. Mater. Sci.*, 1990, **25**, 2655–2666.
20. Cheng, B. L., Gabbay, M., Fantozzi, G. and Duffy, W., Mechanical loss and elastic modulus associated with phase transitions of barium titanate ceramics. *J. Alloys Comp.*, 1994, **211/212**, 352–355.